*Shree H.K. Ranjin, Nidhi Pathak, Charu Lata Dube**

School of Nano Sciences, Central University Gujarat, Gandhinagar, Sector, India

Scientific paper
ISSN 0351-9465, E-ISSN 2466-2585
https://doi.org/10.62638/ZasMat1037

Zastita Materijala 65 (1)
169 - 175 (2024

Photocatalytic degradation of textile dye with titanium (IV) doped tungsten oxide nanoparticles

ABSTRACT

Water pollution from textile industries is a major concern with respect to the availability of clean drinking water. The removal of textile (organic) dyes through photocatalytic degradation with pure WO_3 and titanium (IV) doped tungsten oxide [Ti (IV)-WO_3] nanospheres were studied under visible light. The WO_3 and Ti (IV)-WO_3 nanospheres were synthesized via microwave-assisted method at microwave power of 160 W for the duration of 20 mins. The as synthesised WO_3 and Ti (IV)-WO_3 nanospheres were characterized for their structural, microstructural, and spectroscopic properties by using powder X-ray diffraction (XRD), UV–Visible (UV-Vis) spectroscopy, Fourier-transform infrared spectroscopy (FTIR), Scanning electron microscopy (SEM) and High-resolution transmission electron microscopy (HR-TEM). The X-ray diffractograms confirmed the formation of highly pure WO_3 and Ti (IV)-WO_3 nanospheres. The average crystallite size of WO_3 and Ti (IV)-WO_3 nanospheres were calculated as 53.37 nm and 35.24 nm respectively using Debye Scherrer equation. The bandgap of Ti (IV)-WO_3 was found to be decreased to 2.5 eV from 3.2 eV (WO_3) respectively. It can be deduced that Ti (IV)-WO_3 can be utilized as efficient visible light (λ>420 nm) driven photocatalyst as the bandgap was < 3 eV. The agglomerated spherical nanoparticles were seen for WO_3 and Ti (IV)-WO_3 in the HR-TEM images. The photocatalytic activity of textile dye was analyzed by UV-Vis spectrophotometer under visible light. The photocatalytic organic dye degradation was investigated. The enhanced photocatalytic activity of titanium (IV) doped tungsten oxide (10 wt%) was observed to be ~100% in 100 mins. This makes titanium (IV) doped tungsten oxide nanospheres, a potential nanomaterial for water purification.

***Keywords**: Photocatalytic degradation, organic dyes, microwave assisted method, photocatalytic activity*

1. INTRODUCTION

In contemporary world, water pollution has a far-reaching negative consequence in the ecosystem. The harmful effluents in water includes broadly organic and inorganic wastes such as dyes, pharmaceutical ingredients, pesticides, fertilizers, heavy metal ions, metal oxides and metal complexes etc. Several industries such as the textiles, paper, chemicals, fertilizers, pesticides, metal-plating, batteries, food processing, refineries and pharma industries are the source of uncontrolled water pollution [1].

*Corresponding author: Charu Lata Dube
E-mail: charulata.dube@cug.ac.in
Paper received: 27. 09. 2023.
Paper accepted: 13. 12. 2023.
Paper is available on the website: www.idk.org.rs/journal

The release of textile dyes (organic pollutants) into the water bodies through textile industries increase the biochemical and chemical oxygen demand (BOD and COD), reduce the growth of the plant, enter the food chain, and may further lead to toxicity, mutagenicity, and carcinogenicity [2]. Hence, several methods have been adopted for the purification of waste water.

The water purification through photocatalysis of dye degradation is highly researched area by several researchers [3,4]. Photocatalysis technique involves, usage of a suitable photocatalyst which degrades the harmful contaminants into simple mineral acids, carbon dioxide and hydrogen in a very short period in the presence of near UV / Visible light [5,6]. Photocatalysts are the solids which accelerate the reaction rate in the presence of light without undergoing any permanent

chemical change throughout the reaction [7]. Among the photocatalysts, the visible-light-driven photocatalysts are extensively utilized for the photochemical induced reactions. The photocatalytic efficiency of photocatalysts under visible light can be enhanced by direct and effective method of band gap regulation. The dopant (cations), into the lattice of the semiconductors alters the band structure of the semiconductors, resulting in the formation of narrow bands which are localized above the valence bands (VB) in the semiconductors which ultimately extend the visible light absorption [8].

The tungsten oxide (WO_3) finds a wide range of applications in photocatalysis which makes it an important semiconductor [9]. It is found that in visible light region, the reduction potential of WO_3 electrons is low as it possesses a low level of conduction band (CB) which enables WO_3 to have low photocatalytic efficiency [10]. The doping of cations such as titanium (Ti^{+4}) ions into the WO_3 lattice will alter its band gap structure and resulting in shift in absorption towards the visible light region.

The particles size of atoms, molecules, or ions, determines the formation of a substitutional solid solution. It is known that the stability of the solid solution depends upon the lesser difference in the particle sizes, and so is the higher solubility of the solution, which is determined by the crystal structure stability [11]. Due to similarity between W^{+6} and Ti^{+4} ionic radii, W-O and Ti-O bond lengths, and WO_3 and TiO_2 crystal structures, Ti^{+4} replaces W^{+6} in the WO_3 lattice. Although W^{+6} and Ti^{+4} have different valences, when Ti (IV) dopes in WO_3, the valence difference between the two causes a finite solid solution to develop [12].

The current research work, describes the synthesis of WO_3 and Ti (IV) doped WO_3 nanospheres through a microwave assisted method for the degradation of Rhodamine B (RhB) dye. Dye degradation efficiency of synthesized photocatalysts were investigated at different concentrations of the dopant [Ti (IV) ions] in the visible light region.

2. EXPERIMENTAL DETAILS

2.1. Materials

Sodium tungstate ($Na_2WO_4.H_2O$, 99%), titanium dioxide (TiO_2, 98%), rhodamine B dye ($C_{28}H_{31}ClN_2O_3$, 96%), nitric acid (HNO_3, 96%) are purchased from Merck. Analytical grade chemicals and reagents are used in purified form. Distilled water (DI) water used, is filtered by a Millipore Milli-Q Integral Water Purification System (Millipore Corp.) throughout the complete experiment.

2.2. Preparation of pure WO_3

A dissolution of 6 g of $Na_2WO_4.H_2O$ in 70 ml of distilled water was prepared and stirred for 15 mins. Addition of a specific concentration of HNO_3, to maintain the pH~1 of the solution. HNO_3 acts as a precipitating agent. The solution turned light yellow in color after the addition of HNO_3, this solution was transferred to a microwave oven (Samsung 28L, MC28A5013AK/TL) and was processed under 160 W for 20 mins. The preparation of WO_3 is expressed in the equation 1 (Eq.1) [13]. A precipitate was obtained in the end of the reaction. DI water was used for washing the precipitate, after centrifugation. The product was kept for drying at 80° C for 12 h in hot air-drying oven. After calcination at 600° C for 5 h, the final product was dried and stored.

2.3. Preparation of Ti (IV) doped WO_3

6 g of $Na_2WO_4.H_2O$ and different molar ratio (2, 5, 10 and 20 wt%) of TiO_2 were dissolved in 70 ml of DI water. Stirring of the solution for 15 mins with addition of suitable amount of HNO_3 to maintain the pH~1 of the solution was performed. A light-yellow color of the solution was obtained after the addition of HNO_3 and was processed in microwave oven under 160 W for 20 mins. The preparation of Ti (IV) doped WO_3 is expressed in the equation 2 (Eq.2). DI water was used for washing the precipitate, after centrifugation. The product was dried at 80° C for 12 h in hot air-drying oven. Further after calcination at 600° C temperature for 5 h, the product was stored.

$$Na_2WO_4 + 2HNO_3 \rightarrow WO_3 + 2NaNO_3 \quad (1)$$

$$Na_2WO_4 + 2HNO_3 + xTi^{+4} \rightarrow xTi{:}WO_3 + +2NaNO_3 \quad (2)$$

2.4. Characterization

The pure WO_3 and Ti (IV) doped WO_3 nanoparticles were characterized for their structural and morphological properties and were investigated for their photocatalytic activity. The X-ray diffractograms of the samples were recorded with X-ray diffractometer (XRD, D8 Advance, Bruker, Germany) with Cu Kα X-ray radiation source in 1.5456 Å at 40 kV and 40 mA over the 2θ range of 10-80° with a scan rate of 0.1 sec/step. The morphological studies were performed with a 180 kV High resolution transmission electron microscope (HR-TEM) (JEOL JEM-2100 TEM, Tokyo, Japan). The TEM samples were prepared on carbon-coated copper grids, followed by drying in air. The optical properties were analyzed with Fourier transform infrared spectrophotometer

(FTIR, Perkin Elmer Spectrum 65 series, Massachusetts, United States) in the range of 400-4000 cm^{-1} and Ultraviolet-Visible spectrophotometer (UV, Shimadzu UV1800 ENG 240V) in the spectral range of 300–800 nm.

2.5. The photodegradation of rhodamine B (RhB) dye

The photocatalytic dye degradation efficiency of both pure WO_3 nanospheres and Ti (IV)-WO_3 nanospheres were determined by using a 200 W incandescent bulb as a visible light source for the degradation of RhB in aqueous solution. The photocatalyst (90 mg of photocatalyst [Ti (IV)-WO_3] was added to RhB aqueous solution ($1x10^{-5}$ M) in a conical flask at 25° C. Stirring of solution was done for 30 mins in dark condition for equilibrium adsorption and desorption. The photocatalytic tests were carried out at different intervals of time by taking 3 ml of suspension each time followed by centrifugation (6000 rpm, 5 mins). The degraded RhB concentration was measured using obtained photocatalyst and supernatant after centrifugation. The concentrations of RhB were measured with the UV-Visible spectrophotometer.

3. RESULTS AND DISCUSSIONS

3.1. XRD analysis

The X-ray diffractograms of WO_3 and Ti (IV)-WO_3 are shown in Fig.1.The XRD peaks in Fig.1(a) at 23°, 23.5°, 24.3° correspond to the WO_3 phase with (002), (020) and (200) planes, respectively (JCPDS File No. 01-072-1465) [14]. The Fig.1(a) shows XRD pattern of pure WO_3 and the XRD patterns of Ti (IV)-WO_3 with doping of Ti (IV) as 2, 5, 10, 20 wt% are shown in Fig.1(b), 1(c), 1(d) and 1(e), respectively. The average crystallite size of WO_3 nanospheres is calculated as ~ 53.3 nm using Debye Scherrer equation (Eq.3).

$$d = K\frac{\lambda}{\beta\, Cos\, \theta} \qquad (3)$$

Where

d average crystallite size,

K shape constant (0.9),

λ wavelength (1.54 Å),

β full width at half maxima,

θ Bragg's angle of respective peaks.

The doping of Ti (IV) is confirmed with the peak values obtained at 25.2°, 37.7º, 48.1°, 55.1º, and 62.7. The obtained 2θ values confirm the presence of TiO_2 anatase phase with characteristic peak at 25.2°, corresponding to the (101) plane in Fig.1(b, c, d, e) (JCPDS File No. 75-1537) [15]. The increment in the Ti (IV) concentration led to increase in the intensity of the peak at 25.2° gradually (marked in the Fig.1 with black ellipse). The obtained XRD patterns explain that with the increase in the dopant concentration of Ti (IV) above 10 wt%, a separate phase of TiO_2 appears, which indicates that the Ti (IV) ions is doped in the lattice of WO_3 crystal structure to form a finite solid solution.

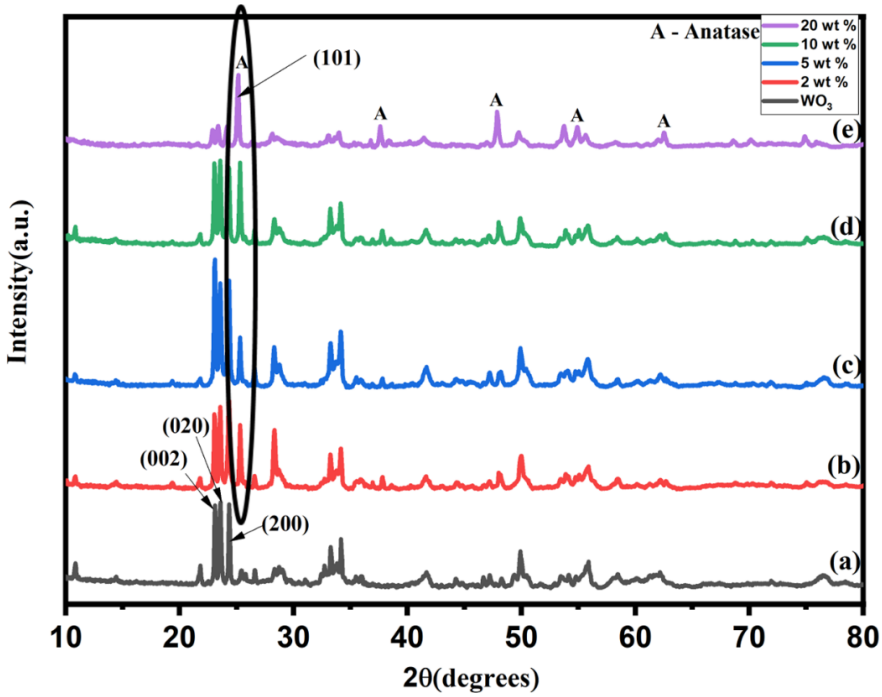

Figure 1. X- ray diffractogram of (a) pure WO_3, (b) 2 wt% Ti (IV)-WO_3, (c) 5 wt% Ti (IV)-WO_3, (d) 10 wt% Ti (IV)-WO_3, (e) 20 wt% Ti (IV)-WO_3 nanoparticles

Slika 1. Rendgenski difraktogram (a) pure WO_3, (b) 2 wt% Ti (IV)-WO_3, (c) 5 wt% Ti (IV)-WO_3, (d) 10 wt% Ti (IV)-WO_3, (e) 20 wt% Ti (IV)-WO_3 nanočestice

3.2. HR-TEM analysis

The corresponding HR-TEM morphology of pure WO_3 and Ti (IV)-WO_3 is shown in Fig.2. Fig.2(a) corresponds to the morphology of pure WO_3 which is nano-spherical in nature with average size of nanoparticles ~5.29 nm. Fig.2(b) represents the similar nano-spherical morphology of Ti (IV)-WO_3 nanoparticles. The HR-TEM images illustrate that WO_3 nanoparticles size is unaffected by the doping of Ti (IV) cations into the lattice. A reduction in the size of the nanoparticles (average size~4.4 nm) is observed after doping of Ti (IV) ions. In addition, doping of titanium may reduce agglomeration of nanoparticles, Fig.2(b) [16].

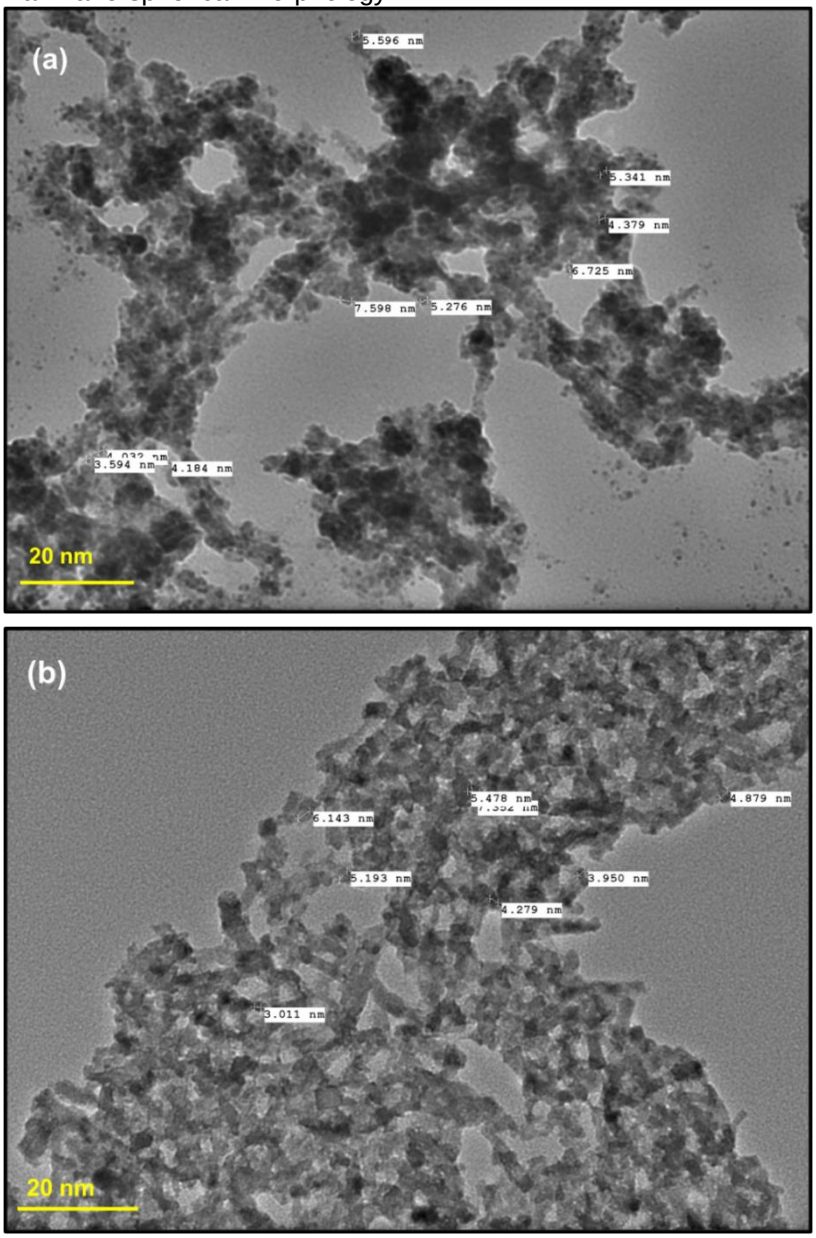

Figure 2. HR-TEM images of (a) pure WO_3 and (b) Ti (IV)-WO_3 nanoparticles

Slika 2. HR-TEM slike (a) pure WO_3 and (b) Ti (IV)-WO_3 nanočestice

3.3. FTIR analysis

The FTIR analysis is performed for pure WO_3 and Ti (IV)-WO_3 nanoparticles. Fig.3 represents the FTIR spectrum of (a) pure WO_3 ($2.74x10^{-1}$ M), (b) 2 wt%, (c) 5 wt%, (d) 10 wt%, (e) 20 wt % Ti (IV)-WO_3 nanoparticles, respectively. The FTIR spectra

of WO_3 exhibits peaks at 620 cm^{-1} (W-O stretching) and 831 cm^{-1} (W-O-W bending) as shown in Fig.3(a). Fig.3(b), (c), (d) and (e) represents the absorption peak at 528 cm^{-1} and a small shoulder peak at 1401 cm^{-1} corresponding to the Ti-O-Ti bending and stretching modes, respectively.

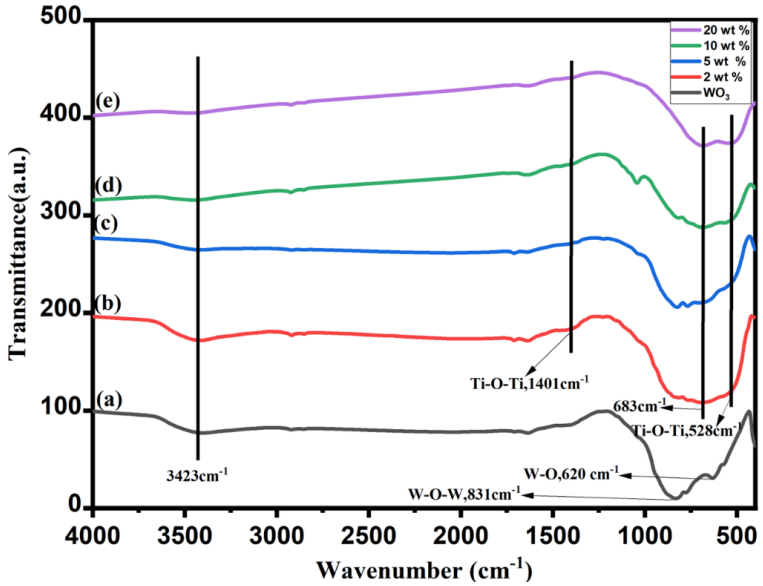

Figure 3. FTIR spectra of (a) pure WO_3, (b) 2 wt% Ti (IV)-WO_3, (c) 5 wt% Ti (IV)-WO_3, (d) 10 wt% Ti (IV)-WO_3, (e) 20 wt% Ti (IV)-WO_3 nanoparticles

Slika 3. FTIR spektar (a) pure WO_3, (b) 2 wt% Ti (IV)-WO_3, (c) 5 wt% Ti (IV)-WO_3, (d) 10 wt% Ti (IV)-WO_3, (e) 20 wt% Ti (IV)-WO_3 nanočestica

The presence of Ti (IV) ions into the lattice of WO_3 is confirmed. The peak broadening with reduction in WO_3 peak intensities is observed with the Ti (IV) ions doping into the lattice of WO_3, Fig.3(b). In Fig.3(e), the appearance of broad peak ~681cm^{-1} distinctly (with the increase in concentration of Ti (IV) ions) can be attributed to the Ti–O–Ti bonds formed in the TiO_2 lattice [17]. This indicates that the Ti (IV) ions is doped in the lattice of WO_3 crystal structure to form a finite solid solution, supporting XRD results. Additionally, the peak observed at ~3423 cm^{-1} is corresponding to hydroxyl group of O-H stretching vibration [18].

3.4. Photocatalytic Degradation study

The photocatalytic performance is examined by photo catalytically degradation of an aqueous solution of RhB dye. The absorption spectra of RhB aqueous solution ($1x10^{-5}$ M, 150 ml) with degradation by 90 mg of photocatalyst (Ti (IV)-WO_3) under the exposure of 200 W tungsten bulb is shown in Fig.4(a).

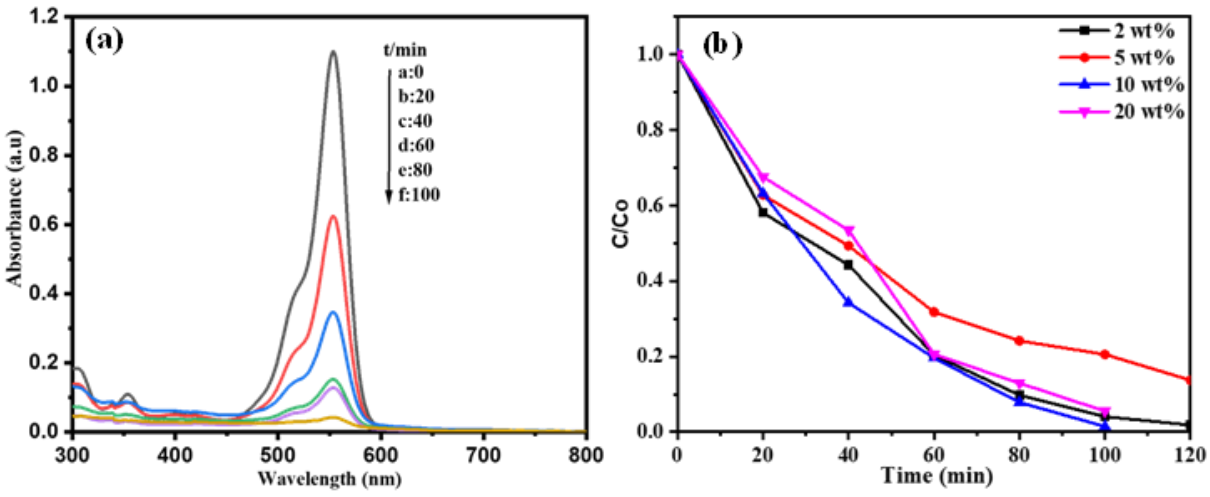

Figure 4.(a) Absorption spectrum of RhB solution with 10 wt% Ti (IV) -WO_3 (b) Photodegradation of RhB with 2 wt%,5 wt%,10 wt% and 20 wt% Ti(IV)-WO_3 photocatalysts

Slika 4. (a) Spektar apsorpcije rastvora RhB sa 10 wt% Ti (IV) -WO_3 (b) Fotodegradacija RhB sa 2 tež%, 5 tež%, 10 tež% i 20 tež% Ti(IV)-WO_3 fotokatalizator

The absorption peak at 550 nm was obtained, corresponding to the absorption of RhB molecules [19]. The rapid decrease in the intensity of the absorption peak was observed with the continuous exposure time and the disappearance in the peak is observed after 100 mins. In the presence of visible light, a series of comparative experiments were performed, to investigate the influence of concentration of Ti (IV) ions. It was observed from Fig.4(a) that in the absence of any photocatalyst, RhB is almost not degraded. It was observed that the photocatalytic efficiency is almost 100% with 120 mins of visible light irradiation in 2 wt% Ti (IV)-WO_3.

The degradation efficiency reduced to ~86% after 120 mins of visible light irradiation with 5 wt% Ti (IV)-WO_3. The doping of 10 wt% Ti (IV)-WO_3 exhibits good photocatalytic activity and dye degradation efficiency reaches almost 100% in 100 mins of visible light irradiation. However, an excess amount of Ti (IV) ions in WO_3 results in decrease of degradation efficiency of ~94% in 100 mins of light irradiation. Thus, it can be inferred that 20 wt% doped Ti (IV)-WO_3 nanoparticles exhibits a low photocatalytic efficiency than its 10 wt% doped counterpart within 100 mins. Therefore, excessive doping of Ti (IV) ions is not preferable [20].

Hence, the above results reveal that the photocatalytic activity of Ti (IV) doped WO_3 nanoparticles is improved in comparison to the pure WO_3 photocatalyst. The optimized percentage of Ti (IV) dopant is 10 wt%. Although, the amount of Ti (IV) with 20 wt%, the photocatalytic activity of the Ti (IV) doped WO_3 photocatalyst decreases.

4. CONCLUSION

In summary, we reported a facile method for synthesis of pure WO_3 nanospheres and Ti (IV)-WO_3 nanospheres. The doping of Ti (IV) ions reduced the band gap of WO_3 to form additional impurity states in the band structure of WO_3. The presence of Ti (IV) ions into the lattice of WO_3 was confirmed with several characterizations performed. The morphology of Ti (IV)-WO_3 as nanospheres confirmed that doping had no effect on the morphology of WO_3 nanoparticles. The photocatalytic activity obtained of Ti (IV)-WO_3 nanoparticles proved that the photocatalytic efficiency improved with the doping of Ti (IV) ions. This research suggests a suitable route for the synthesis of photocatalysts in short time with enhanced properties. The improved visible light driven photocatalytic activity of Ti (IV)-WO_3 nanoparticles paves a way for its application in the water purification.

Acknowledgements

The authors are grateful to the Central Instrumentation Facility (CIF), Central University of Gujarat (CUG), Gandhinagar, Gujarat, India for providing necessary research facilities and support. Ms. Shree Ranjini H.K. thankfully acknowledges Dr. Charu Lata Dube the for conceptualizing the work. Ms. Shree Ranjini H.K. acknowledges Ms. Nidhi Pathak and Ms. Ritu Kumari Pilania for their guidance and scientific discussion during the work.

5. REFERENCES

[1] R.Gusain, K.Gupta, P.Joshi, O.P.Khatri (2019) Adsorptive removal and photocatalytic degradation of organic pollutants using metal oxides and their composites: A comprehensive review, Advances in colloid and interface science, 272, 102009.

[2] B.Lellis, C.Z.Fávaro-Polonio, J.A.Pamphile, J.C. Polonio (2019) Effects of textile dyes on health and the environment and bioremediation potential of living organisms, Biotechnology Research and Innovation, 3(2), 275-290.

[3] M.Saeed, M.Muneer, A.U.Haq, N.Akram (2022) Photocatalysis: An effective tool for photo-degradation of dyes—A review, Environmental Science and Pollution Research, p.1-19.

[4] A.Rafiq, M.Ikram, S.Ali, F.Niaz, M.Khan, Q.Khan, M.Maqbool (2021) Photocatalytic degradation of dyes using semiconductor photocatalysts to clean industrial water pollution, J. of Industrial and Engineering Chemistry, 97, 111-128.

[5] M.Elangovan, S.M.Bharathaiyengar, J.Ponnan Ettiyappan (2021) Photocatalytic degradation of diclofenac using TiO_2-CdS heterojunction catalysts under visible light irradiation, Environmental Science and Pollution Research, 28, 18186-18200.

[6] H.Yuan, Y.Zhu, Q.Xu (2020) Research Progress of Bi-Based Catalysts for Photocatalytic Oxidation of VOCs, Hans Journal of Chem. Engin. and Techn., 10(2), 73-81.

[7] [N.A.Rajpurohit, K.Bhakar, M.Nemiwal, D.Kumar (2022) Design and synthesis of hybrid nanostructures for sustainable energy and environmental remediation, Arabian Journal of Geosciences, 15, 1-16.

[8] C.Feng, S.Wang, B.Geng (2011) Ti (iv) doped WO_3 nanocuboids: fabrication and enhanced visible-light-driven photocatalytic performance, Nanoscale, 3(9), 3695-3699.

[9] F.Heshmatpour, F.S.Seyed Atashi (2023) Synthesis and characterization of iron-based spinel nanoparticles with different coatings and their ability in photocatalytic degradation of methylene blue, J. of Applied Chemistry, 18(68), 9-28.

[10] T.L.Nguyen, V.D.Quoc, T.L.Nguyen, T.T.T.Le, T.K.Dinh, P.H.Nguyen (2021) Visible-Light-Driven SO_4^{2-}/TiO_2 Photocatalyst Synthesized from Binh Dinh (Vietnam) Ilmenite Ore for Rhodamine B Degradation, J. of Nanomaterials, 2021, 1-13.

[11] U.Aarthi, D.Shukla, S.Rengaraj, K.S.Babu (2020). Ordered to defect fluorite structural transition in $Ce_{1-x}Nd_xO_{2-\delta}$ system and its influence on ionic conductivity, J. of Alloys and Compounds, 838, 155534.

[12] K.Yin, Y.Shen (2020) Theoretical insights into CO_2 hydrogenation to HCOOH over $Fe_xZr_{1-x}O_2$ solid solution catalyst, Applied Surface Science, 528, 146926.

[13] N.Moghni, H.Boutoumi, H.Khalaf, N.Makaoui, G.Colón (2022) Enhanced photocatalytic activity of TiO_2/WO_3 nanocomposite from sonochemical-microwave assisted synthesis for the photodegradation of ciprofloxacin and oxytetracycline antibiotics under UV and sunlight, J. of Photochemistry and Photobiology A: Chemistry, 428, 113848.666.

[14] H.Ijadpanah-Saravy, M.Safari, A.Khodadadi-Darban, A.Rezaei (2014) Synthesis of titanium dioxide nanoparticles for photocatalytic degradation of cyanide in wastewater, Analytical Letters, 47(10), 1772-1782.

[15] I.A.De Castro, J.A.De Oliveira, E.C.Paris, T.R. Giraldi, C.Ribeiro (2015) Production of heterostructured TiO_2/WO_3 Nanoparticulated photocatalysts through a simple one pot method, Ceramics International, 41(3), 3502-3510.

[16] C.H.Su, C.Y.Su, Y.F.Lin (2015) Microstructural characterization and field emission properties of tungsten oxide and titanium-oxide-doped tungsten oxide nanowires, Materials Chemistry and Physics, 153, 353-358.

[17] B.Singaram, J.Jeyaram, R.Rajendran, P. Arumugam, K.Varadharajan (2019) Visible light photocatalytic activity of tungsten and fluorine codoped TiO_2 nanoparticle for an efficient dye degradation, Ionics, 25, 773-784.

[18] J.Y.Zhang, I.W.Boyd, B.J.O'sullivan, P.K.Hurley, P.V.Kelly, J.P.Senateur (2002) Nanocrystalline TiO_2 films studied by optical, XRD and FTIR spectroscopy, J. of Non-Crystalline Solids, 303(1), 134-138.

[19] S.A.Singh, G.Madras (2013) Photocatalytic degradation with combustion synthesized WO_3 and WO_3TiO_2 mixed oxides under UV and visible light, Separation and Purification Technology, 105, 79-89.

[20] İ.Ç.Davaslıoğlu, K.V.Özdokur, S.Koçak, Ç.Çırak, B.Çağlar, B.B.Çırak, F.N.Ertaş (2021) WO_3 decorated TiO_2 nanotube array electrode: Preparation, characterization and superior photoelectrochemical performance for rhodamine B dye degradation, J. of Molecular Structure, 1241, 130673.

IZVOD

FOTOKATALITIČKA DEGRADACIJA TEKSTILNE BOJE SA NANOČESTICAMA VOLFRAM OKSIDA DOPOVANIM TITANIJUMOM (IV)

Zagađenje vode iz tekstilne industrije predstavlja veliku zabrinutost u pogledu dostupnosti čiste vode za piće. Uklanjanje tekstilnih (organskih) boja fotokatalitičkom degradacijom sa čistim VO_3 i titanijumom (IV) dopiranim volfram oksidom [Ti (IV)-VO_3] nanosferama je proučavano pod vidljivom svetlošću. Nanosfere VO_3 i Ti (IV)-VO_3 su sintetizovane metodom uz pomoć mikrotalasa pri mikrotalasnoj snazi od 160V u trajanju od 20 minuta. Sintetizovane nanosfere VO_3 i Ti (IV)-VO_3 su okarakterisane po svojim strukturnim, mikrostrukturnim i spektroskopskim osobinama korišćenjem difrakcije rendgenskih zraka na prahu (XRD), UV-Visible (UV-Vis) spektroskopije, Fourier-transform infracrvene spektroskopije (FTIR), skenirajuća elektronska mikroskopija (SEM) i transmisiona elektronska mikroskopija visoke rezolucije (HR-TEM). Rendgenski difraktogrami potvrdili su formiranje visoko čistih nanosfera VO_3 i Ti (IV)-VO_3. Prosečna veličina kristalita VO_3 i Ti (IV)-VO_3 nanosfera je izračunata kao 53,37 nm i 35,24 nm respektivno korišćenjem formule Debie Scherrer. Utvrđeno je da je pojasni razmak Ti (IV)-VO_3 smanjen na 2,5 eV sa 3,2 eV (VO_3) respektivno. Može se zaključiti da se Ti (IV)-VO_3 može koristiti kao efikasan fotokatalizator koji pokreće vidljiva svetlost (l>420 nm), pošto je pojas bio < 3eV. Aglomerirane sferične nanočestice su viđene za VO_3 i Ti (IV)-VO_3 na HR-TEM slikama. Fotokatalitička aktivnost tekstilne boje je analizirana UV-Vis spektrofotometrom pod vidljivom svetlošću. Istražena je fotokatalitička organska degradacija boje. Uočeno je da je povećana fotokatalitička aktivnost volfram oksida dopiranog titanijumom (IV) (10 tež.%) ~100% za 100 minuta. Ovo čini nanosfere volfram oksida dopirane titanijumom (IV), potencijalnim nanomaterijalom za prečišćavanje vode.

Ključne reči: *fotokatalitička degradacija, organske boje, mikrotalasna metoda, fotokatalitička aktivnost*

Naučni rad
Rad primljen: 27.09.2023.
Rad prihvaćen: 13.12.2023.
Rad je dostupan na sajtu: www.idk.org.rs/casopis